Production procedures and mechanical behaviour of interlocking stabilized compressed earth blocks (ISCEBs) manufactured using float ram 1.0 press

Contents lists available at GrowingScience

Engineering Solid Mechanics

homepage: www.GrowingScience.com/esm

Production procedures and mechanical behaviour of interlocking stabilized compressed earth blocks (ISCEBs) manufactured using float ram 1.0 press

Mauro Sassu[a*], Antonio Romanazzi[b], Linda Giresini[c], Walter Franco[d], Carlo Ferraresi[d], Giuseppe Quaglia[d] and Elisa Orefice[e]

[a]*Department of Civil, Environmental Engineering and Architecture, Università di Cagliari, Italy*
[b]*Department of Civil Engineering, Universidade do Minho, Portugal*
[c]*Department of Energy, Systems, Territory and Constructions Engineering, Università di Pisa, Italy*
[d]*Department of Mechanical and Aerospace Engineering, Politecnico di Torino, Italy*
[e]*Technical Engineer, Comune di Montescudaio, Italy*

ARTICLEINFO

Article history:
Received 22 September, 2017
Accepted 10 January 2018
Available online
18 March 2018

Keywords:
Earth blocks
Human power
Mechanical test
Production test
Floating RAM press

ABSTRACT

This paper illustrates an innovative manufacturing procedure for producing handcrafted interlocking stabilized compressed earth blocks (ISCEBs). A comparison of the mechanical properties of ISCEBs is conducted to assess the influence of varying components. The ISCEBs are manufactured by employing different block densities with three distinct mixtures (earth, earth and lime, earth and straw) and by using a human-powered machine named Float RAM 1.0 Press. The manual press was conceived for regions with limited access to technology and allows the production of interlocking blocks via two modes of compaction: mono-directional and bi-directional. A production average of approximately 30 blocks/hour corresponding to the work of three people is achieved. Three-point bending tests and uniaxial compression tests are carried out to investigate the ISCEB mechanical behaviour. The improvements obtained by incorporating additives into the subset of ISCEBs made from a pure earth mixture are tested. The aim of this work is to identify, for this specific technology, the relationship between production parameters and the consequent behaviour of different stabilization methods. A correlation is found between the compaction force and the compression strength of ISCEBs. The addition of lime increases strength and causes the blocks to exhibit a brittle behaviour. Moreover, the incorporation of straw fibres improves the tensile strength and ductility without significantly affecting the compression strength of the blocks. Energy-based parameters are obtained for all the tests, allowing the assessment of the ISCEB mechanical and dissipation properties.

1. Introduction

In the field of sustainable development, there is an increasing interest in constructive procedures characterized by appropriate technologies and low-cost materials (Niroumand et al., 2013; Maskell et al., 2016; Franco et al., 2016, 2017; Sassu et al., 2016 a,b). In particular, the focus on raw earth as a material for civil constructions is promoted by its recyclability, local availability, environmental sustainability, low cost and ease of use. Raw earth structures also permit self-construction approaches, especially in developing countries (Pacheco-Torgal & Jalali, 2012; Arumala & Gondal, 2007; Mukerji, 1988; Houben & Guillaud, 1989; Oppong & Badu 2012). Furthermore, the thermal mass of raw earth, due to the capacity of earth constructions to regulate the interior temperature and humidity, is attractive

* Corresponding author.
E-mail addresses: msassu@unica.it (M. Sassu)

doi: 10.5267/j.esm.2018.3.004

as a means to reduce the building energy demand (Delgado & Guerrero 2006). These aspects are emphasized by the growing demand for housing in underdeveloped countries. Local resources cannot ensure the extensive applicability of modern construction techniques; thus, raw earth construction techniques can represent sustainable and reasonable solutions from an economic point of view.

The resistance of earth blocks is usually low; in fact, in most cases, the compression strength is lower than 1 MPa. However, these values can be sufficient for many practical cases, particularly for the low-rise buildings found throughout rural areas or cities in developing countries (Guillaud & Houben, 1994; Milke, 2006). The compressed earth blocks (CEBs), which originated in the mid-twentieth century, represent a technological innovation among the raw earth techniques (e.g., rammed earth, adobe, and cob). In the CEB technique, the earth mixture is compacted using motor-powered or manual presses (Reddy 2015). The mentioned tools ensure an improvement in production quality control due to the possibility to regulate the pressure during the production of blocks. Quality control during or after production is a crucial issue especially for the manual production undertaken in developing countries. Consequently, the idea of promoting human-powered machines, which are easy to provide and to use, is of remarkable interest. The mixture compaction mode can be differentiated as mono- or bi-directional, with a unique or opposing coupled movable mould, respectively (Ferraresi et al., 2011).

A large number of experimental studies that evaluate the mechanical and thermal properties of earth blocks are available in the literature (Bui et al., 2009; Bouhicha et al., 2005; Kouakou & Morel, 2009). Traditional tests, such as three-point bending or compression tests, are illustrated in (Morel et al., 2007 Morel & Pkla, 2002), where new testing methods are also proposed. In this manner, a proper classification of blocks after production and curing is possible depending on their mechanical properties.

To improve the durability and mechanical performances of earth blocks, stabilization via the addition of sand, lime, fibres or other components plays a delicate role during the production phase. The efficiency of stabilization also depends on the type and amount of compaction force (Walker, 1995; Billong et al., 2009; Anifowose, 2000; Venkatarama Reddy et al., 2016).

Several studies have focused on evaluating the effects of the addition of fibres, which was generally carried out to enhance the tensile strength and ductility of the blocks (Delgado & Guerrero, 2006; Bati, 2001; Parisi et al., 2015; Lenci et al., 2011). The positive role of fibres has also been confirmed by analyses of the use of recycled waste materials, e.g., plastic fibres or cellulose-based binders (Gomes Battistelle & Borges Faria, 2005; Varadarajan & Govindan, 2013). Furthermore, it has been shown that stabilization using sand influences not only the mechanical but also physical properties of blocks and their ageing time (Pekmezci et al., 2012; Binici et al., 2005, 2007). Other authors have analysed the use of stabilized CEBs for affordable high-quality dwellings (Matta et al., 2015) or the addition of granitic soils to improve the mechanical properties of the units (Oliveira et al., 2016; Silva et al., 2015). Recent investigations on the behaviour of walls made using interlocking stabilized compressed earth blocks (ISCEBs) (Laursen et al., 2015; Qu et al., 2015 a,b) and the role of the compaction force (Bruno et al., 2017) have been carried out; in particular, the adoption of interlocking dry-stack blocks (Sturm et al., 2015) can simplify the execution phases. When this type of building exhibits box-type behaviour, the role of the out-of-plane behaviour must be evaluated in the seismic context (Qu et al., 2015 a,b; Andreini et al., 2013) or with regard to rocking phenomena in masonry walls (Giresini & Sassu, 2017; Giresini et al., 2016). Indeed, earth block walls behave as rigid blocks that can rotate in the case of dynamic actions. However, few research works on the mechanical performances of individual ISCEBs are available; therefore, the present study attempts to contribute to this field. The innovative aspects of this paper include the use of human power to operate a float ram press machine with bilateral actions to produce ISCEBs. Another aspect is the proposal of a suitable method for producing an efficient earth block in terms of self-construction in low technology areas via a manual press. In fact, this research is conducted in collaboration with a self-construction pilot project in the village of Kouini (Burkina Faso). A third contribution regards the comparison of experimental results for blocks with several additives

(lime, straw fibres, only soil), with several masses (6.4, 6.6, 6.8 kg/block) and that undergo several actions during production (bi- and mono-lateral actions).

First, a geotechnical analysis of the soil used is illustrated in Section 2. Then, the production process of twelve series of six blocks is described. The production makes use of the Float RAM 1.0 manual press. The results of three-point bending (Section 3) and compression (Section 4) tests are then presented. Finally, specific energy parameters are proposed to possibly use the results in energy-based approaches for the dynamic analysis of masonry structures (Giresini, 2015). These parameters are designed to highlight the characteristics of earth blocks in terms of inelastic behaviour and dissipated energy.

2. Production of ISCEBs

2.1. Selection of soil and production process

To identify suitable soil for the production of earth blocks, the particle sizes and Atterberg's indices of three samples of soil taken from a cave in Rosignano Marittimo (Leghorn, Italy) were determined by following the ASTM D4318 and ASTM D422 rules. By considering the geotechnical results, sample n° 792 was selected (Table 1) to produce the set of ISCEBs. First, the soil was dried in an oven at 70°C for 24 hours; since the available soil was mainly clayey, the addition of a sand fraction with a diameter between 125 μm and 250 μm was done preliminarily. The amount of sand needed was determined after several different attempts with some pilot samples by following the indications given in (Lenci et al., 2011). Thus, the granulometric mix proportions are given in volumetric units, as displayed in Table 2.

Table 1. Geotechnical properties of tested soils

	Kouini	N° 792	N° 793	N° 794
Gravel %	8.8	0.2	0.0	0.1
Sand %	36.2	13.0	10.0	8.4
Silt %	37.9	52.6	50.0	52.7
Clay %	17.1	34.2	40.0	38.8
Liquid Limit	28	52	59	63
Plastic Limit	19	28	32	32
Plasticity Index	9	24	27	31

Table 2. Granulometric mix design

	N°792		Add	Final	
	kg	%	kg	kg	%
Sand	1.51	13.0	14.50	16.01	61.4
Silt	6.10	52.6	-	6.10	23.4
Clay	3.98	34.2	-	3.98	15.2

Compaction of the mixture was performed by using the Float RAM 1.0 manual press designed by the team at the Department of Mechanical and Aerospace Engineering, Politecnico di Torino (Ferraresi et al., 2014). The press is manually actuated by a lever integrated with a cam matched to a roller hinged to the framework. Rotation of the cam, which is hinged to the strut of a lower plate connected to the framework integral shaft, causes vertical movement of the lower plate, while the upper one is fixed (Fig. 1). The mould of this press is of floating type. Due to the friction between the mixture and the mould, the latter can translate vertically along the same shaft of the framework. This device allows a bi-directional translation of both the upper and lower plates (double effect in Fig. 1), achieving a better distribution of pressure within the height of the block during the compaction phase: the pressure acting from both sides reduces the compaction path along the vertical direction. Moreover, a mono-directional translation can be implemented to lock the movement of the mould (single effect in Fig. 1). The first

innovative aspect of the utilized CEB manual press is the employment of a floating mould. It can translate freely along the pressing direction, automatically balancing the pressure on the upper and lower surfaces of the block and moving only one plate. Unlike the human-powered press available on the market, in the present Float RAM, the bi-directional compression is generated by moving only the lower plate. Since the mould is free to translate, during compression, it moves upwards to equalize the compression force on the top and bottom brick surfaces in the case of null friction between the mould and the frame. The actuation mechanism of the compression plate is then considerably simplified.

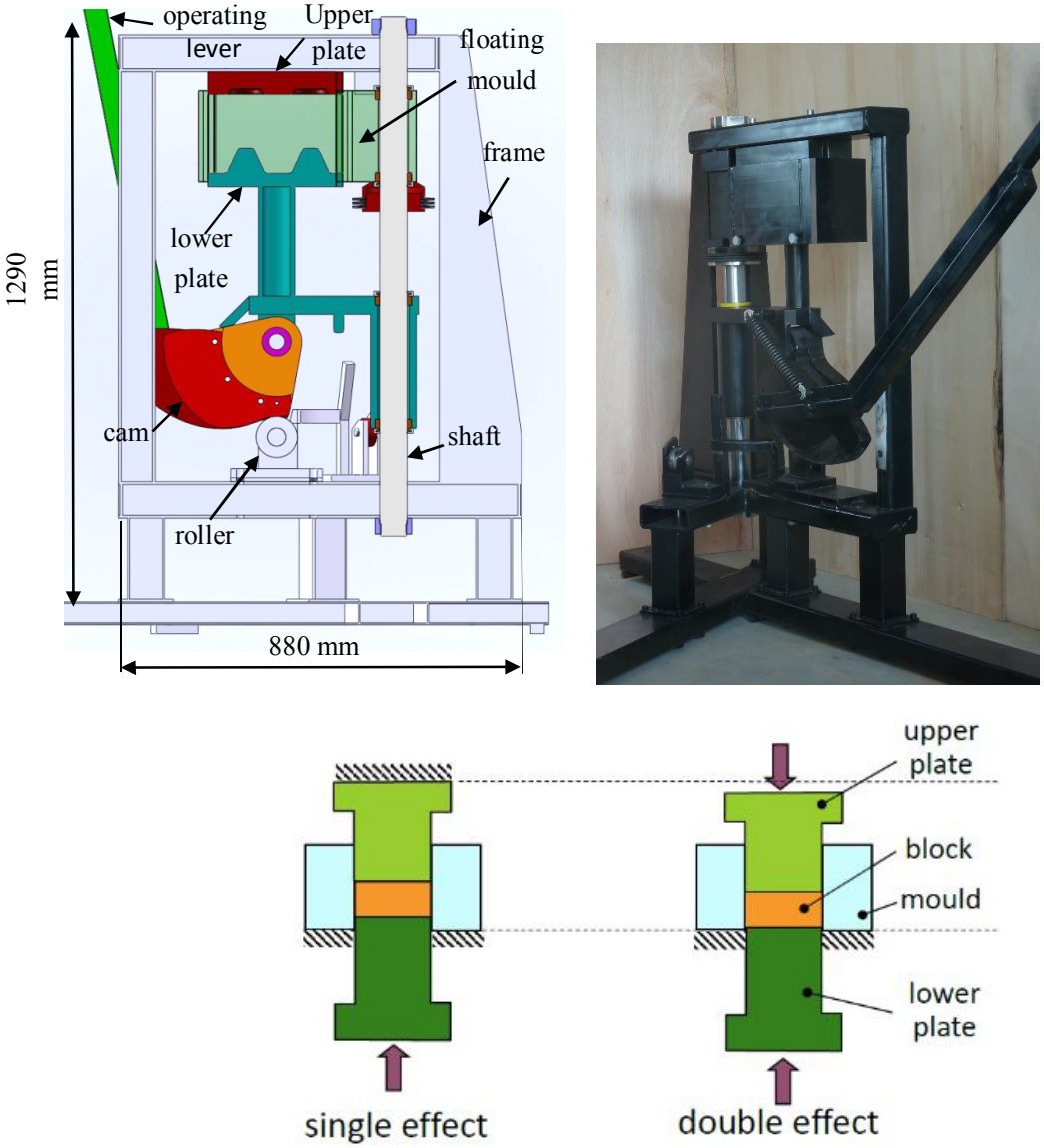

Fig. 1. Float Ram Press 1.0

In addition, the Float RAM is able to maintain a constant worker operating force during the block pressing phase. This is possible because a cam-follower mechanism that can generate the appropriate output function, once the mechanical properties of the earth are known, is used. Finally, to simplify the entire press mechanical architecture, the movements of the members of the press are concentrated in a single node. A single shaft drives the displacement of the lower compression plate during the block forming/block extraction operation and the floating of the mould during the block pressing phase and allows the press configuration to be changed via rotation of the group comprising the lower plate and the floating mould.

This press produces the typical "blocco Mattone" unit, which consists of a 280x140x95 mm^3 block with two cylindrical holes 80 mm in diameter and 55 mm in height. The specific interlocking geometry simplifies the construction procedures of masonry panels, reducing the use of lime and allowing the production of robust walls even when employing thin mortar joints (Mattone, 2001; Melo et al., 2011). For the investigation, the ISCEB series was produced via two compaction modalities: mono-directional (NF series) and bi-directional (F series) compression. Several mix designs were prepared: only soil (T series); soil with the addition of 0.5% straw fibres (weight of the fibre is with respect to the dry weight of soil) with a length of 5-20 mm (P series), following the indications in Millogo et al. (2015) for the Burkina Faso experiments and in Parisi et al. (2015) for the Italian tests; and soil with the addition of 10% lime (weight of lime with respect to the dry weight of soil) (C series), based on indications by Pekmezci et al. (2012). This last mixture is preferred for soils with a plastic index above 15 (Guettala et al., 2002; Osula, 1996).

To achieve suitable compaction, different soils, sands, water ratios and mixture masses were tested, with two optimal ISCEB masses identified: 6.6 kg for the W series and 6.8 kg for the X series. Meanwhile, the mortar workability was determined, with a water amount of approximately 33% of the dry soil mass. A further series of samples with a mass of 6.4 kg (S series) was manufactured due to difficulty in compacting the mixture with fibres. In total, twelve series of samples were produced by combining different compaction modalities (N-NF series), mixture types (T-C-P series) and mixture amounts (W-X-S series) (Table 3). Each series included six units; therefore, a total of 72 specimens were tested.

Table 3. Summary of the produced series

CEB n.	Series	Mixture	Weight	Compaction mode
1-6	TWF	Only soil	6.6 kg	Floating mode
7-12	TWNF	Only soil	6.6 kg	Non-Floating mode
13-18	TXF	Only soil	6.8 kg	Floating mode
19-24	TXNF	Only soil	6.8 kg	Non-Floating mode
25-30	CWF	Soil and lime	6.6 kg	Floating mode
31-36	CWNF	Soil and lime	6.6 kg	Non-Floating mode
37-42	CXF	Soil and lime	6.8 kg	Floating mode
43-48	CXNF	Soil and lime	6.8 kg	Non-Floating mode
49-54	PWF	Soil and straw fibers	6.6 kg	Floating mode
55-60	PWNF	Soil and straw fibers	6.6 kg	Non-Floating mode
61-66	PSF	Soil and straw fibers	6.4 kg	Floating mode
67-72	PSNF	Soil and straw fibers	6.4 kg	Non-Floating mode

T= only soil; P = with straw fibers; C = with lime
S = reduced mass (6.4 kg); W = normal mass (6.6 kg); X = superior mass (6.8 kg)
F = bi-direct. compaction; NF = mono-direct. compaction

The press is equipped with a load cell (capacity: 10^5 N, non-linearity < 0.15% of the rated output, repeatability < 0.10% of the rated output) and a linear potentiometer (capacity: 100 mm, independent linearity < 0.10% of the rated output) that yield the compression force related to the displacement of the lower plate. The data were recorded using an LMS-Scadas Mobile recorder with a 100 Hz sampling rate and the LMS-TestLab Rev.8.a software and later elaborated using the Scilab-5.5.2 numerical computation software. Making use of the data, the progress of the compaction pressure on the upper plate related to the density of the ISCEB and the mechanical work for the compression have been outlined. The average and standard deviations of all production parameters are listed in Table 4.

Table 4. Mechanical work for compaction phase, maximum compression force and pressure

	Work (J)		Compaction force (kN)		Pressure (MPa)	
	Mean	S. D.	Mean	S. D.	Mean	S. D.
TWF	491.85	17.65	41.88	0.93	1.07	0.03
TXF	641.48	25.82	53.13	3.35	1.36	0.08
TWNF	513.23	10.04	43.01	1.05	1.10	0.03
TXNF	608.72	37.34	49.61	2.68	1.27	0.07
CWF	473.44	27.08	40.27	1.59	1.03	0.05
CXF	618.69	95.14	49.73	7.77	1.27	0.20
CWNF	368.42	33.75	30.23	2.41	0.77	0.06
CXNF	468.77	24.47	39.15	2.55	1.00	0.06
PSF	575.60	104.23	43.02	8.20	1.10	0.21
PWF	755.92	54.01	57.33	4.09	1.46	0.11
PSNF	386.43	107.98	28.39	9.66	0.72	0.25
PWNF	575.93	65.63	44.80	4.82	1.14	0.12

T= only soil; P = with straw fibers; C = with lime
S = reduced mass (6.4 kg); W = normal mass (6.6 kg); X = superior mass (6.8 kg)
F = bi-direct. compaction; NF = mono-direct. compaction

The production phase involved three people: one dedicated to the preparation of the mixture, one to filling the machine mould, one to operating the manual press (compaction and extraction phases). An average time of 120 sec was needed to produce a single block, including stacking it on a proper surface after production. These values are comparable with the results of similar researchers (Reddy 2015). The blocks were stacked for one month in an area with a temperature of approximately 20°C and a humidity of 50%.

2.2. Discussion of the production phase

The "pressure force - relative displacement" diagram of the mould (an example is displayed in Fig. 2) is considered to assess the degree of uniformity of the production phase. It is relevant to notice the low data dispersion for the complete production of the 72 blocks. Two outliers in the CXF series occurred for blocks CEB40 and CEB41, the pressure forces of which were particularly high, making it difficult to attain the prescribed displacement. A similar behaviour is observed for blocks CEB55 and CEB56 (the correspondence between CEB blocks and series is reported in Table 3). Further minor singularities, in terms of the pressure force, emerged in the blocks with physical stabilization, in particular for the PSF and PSNF series; the latter is shown in Fig. 2. In those series, the dispersion of data likely depended on the difficulties in uniformly distributing the fibres within a block during the preparation of the handcrafted mixture.

As expected, considering the same type of compaction and mixture, i.e., NF-F and T-C-P, respectively, higher amounts of force and mechanical work are needed to compact more mass, particularly if lime or fibres are added. For the same mixture (T-C-P series) and mass (W-X-S series), the compression force and its related mechanical work during production are higher for the floating mould case compared to the non-floating mould case (Table 4): their increments lie between 5% and

20%. This result probably occurs due to the different friction forces in the mixture for bi-directional compaction along the vertical surfaces of the mould. Indeed mono-directional compaction distributes the external force along a vertical path with double the length compared to the bi-directional one, similar to the well-known phenomenon of pre-stressed concrete elements.

The highest compaction forces were used in the case of straw fibres stabilization, where the compaction mode and mass were kept constant. An average increment of approximately 15%, with respect to the lowest values, occurred for lime stabilization. This result is due to the addition of natural fibres: by decreasing the density of the mixture, the force needed to obtain the same block volume increases, assuming the same mixture mass.

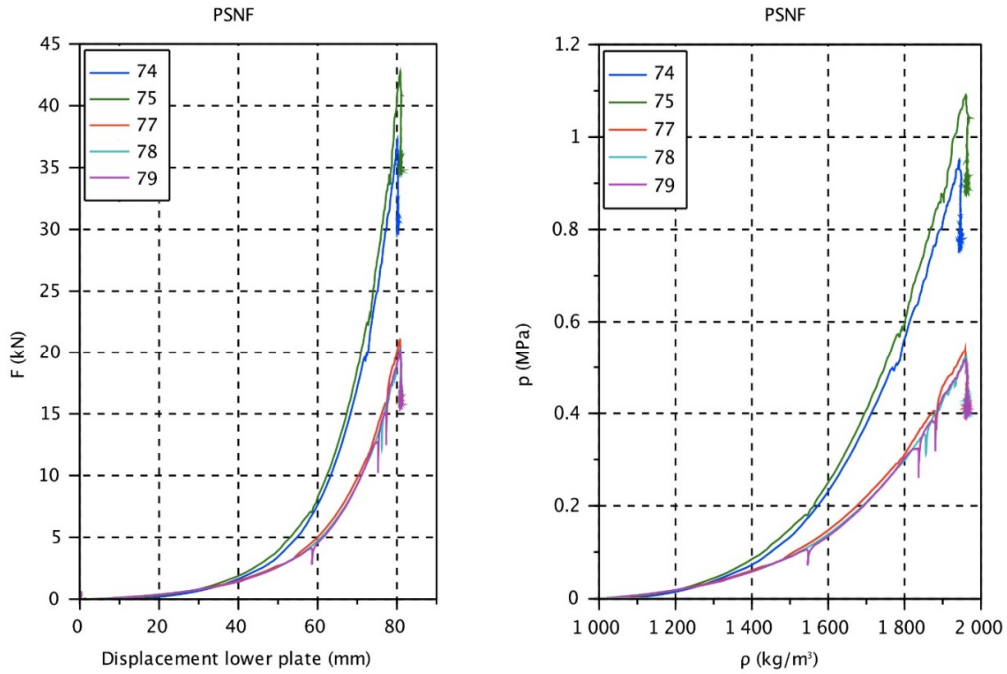

Fig. 2. Force-displacement during production of PSNF series.

3. Three-point bending tests

3.1. Setup of the bending test

In this paragraph, the setup of the bending tests, the aim of which was the determination of the block flexural strength, is illustrated. For this purpose, the procedure proposed in UNI EN 1015-11:2007, which is valid for hardened mortar, was followed. This procedure is valid for prismatic elements such as the block analysed in this paper. Moreover, the inhomogeneous nature of the block is similar to that of hardened mortar. Displacement-controlled three-point bending tests were performed using the Instron model 1186 machine with a displacement rate of 0.5 mm/min and a fixed full-scale force of 500 daN. The span *d* of the bending test was 240 mm. Two potentiometers (tolerance 1 μm) recorded the displacement of the middle section of the blocks on the far end of the crossbeam (Fig. 3). The data were elaborated using the Scilab-5.5.2 numerical computational software. Since the maximum difference between the values of two potentiometers was lower than 0.1 mm, the displacement was calculated as their average. A previous calibration ensured negligible displacements of the faces of the specimen with respect to the extremities of the strain gages (Fig. 3).

Fig. 3. Three points bending test through INSTRON MODEL 1186

The tests revealed an adjustment between the machine and the block for loads up to 20 daN; thus, the initial part of the diagrams was not plotted. Fig. 4a shows a typical diagram of specimen CEB14 of the TXF series (14 is the label of the specimen progressive number). Except for this removal of the initial adjustment of the specimen, neither filtering nor correction of the measurements was introduced in the diagrams. The maximum force F_{max} and the corresponding displacement $x(F_{max})$ are marked. The blocks revealed a negligible residual strength for high displacement values after the peak. The ultimate strength F_u is conventionally assumed as $0.3\ F_{max}$ with the corresponding ultimate displacement x_{Fu}. To evaluate the mechanical properties while achieving a simple interpretation of the experimental results, an energy-based analysis was performed. In particular, the following conventional parameters were considered:

- E_1, elastic energy, given by the area of the force-displacement diagram up to F_{max};
- E_2, post-elastic energy, given by the area of the force-displacement diagram beyond F_{max} up to x_u;

- E_3, ideal post-elastic energy, given by the area of the rectangle in the force-displacement diagram between F_{max} and x_u;
- $P_{F,1} = \frac{E_2}{E_1}$, the ratio of dissipated to elastic energy, identifying the capability to absorb energy;
- $P_{F,2} = \frac{E_2}{E_3}$, the ratio of dissipated to elastic-plastic energy, measuring the level of ductility of the block;
- $\lambda_F = \frac{E_3}{E_1}$, the ideal ductility factor in terms of energy.

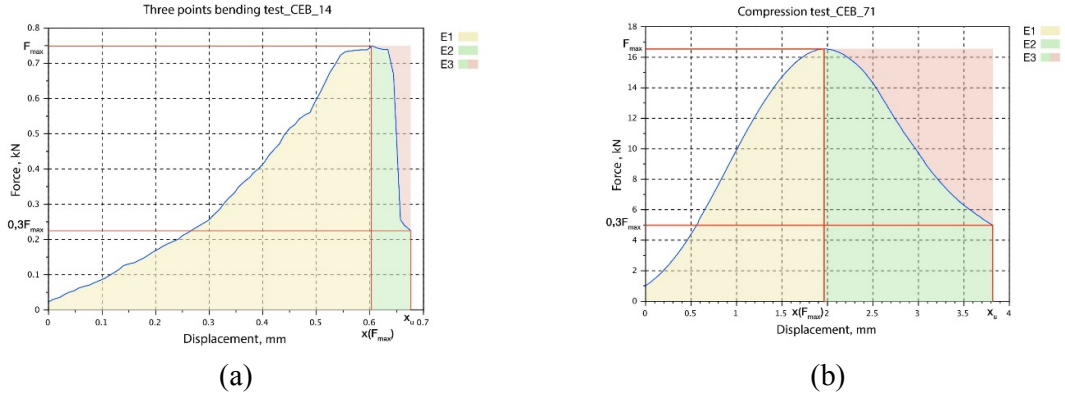

(a) (b)

Fig. 4. Typical diagrams of the mechanical tests: (a) bending test; (b) compression test

Fig. 5. Details of bending collapse of P series (straw fibers reinforcement)

The mentioned dimensionless parameters can support the interpretation of the experimental results, making them suitable for practical application, e.g., for the dynamic analysis of masonry buildings (Giresini, 2015). $P_{F,1}$ is a positive quantity; a zero value indicates a perfect brittle behaviour, and increasing values imply stronger capabilities to display post-elastic energy. $P_{F,2}$ is a quantity between zero and 1; the latter value indicates perfect elastic-plastic behaviour, while the former indicates perfect brittle behaviour. Finally, λ_F is a quantity that conventionally defines the ductility of perfect elastic-plastic behaviour; the corresponding conventional ductility of the specimen can be given by the product

$\lambda_F\ P_{F,2} = P_{F,1}$. All the ISCEBs revealed a yield point under a load of approximately 75 daN, followed by displacement with a constant load, and then a hardening path leading to the peak value. The data dispersions of the T and C series are limited, with the exception of a few outliers. A higher dispersion was found mainly in the post-peak phase of the P series, which occurred due to the high variability of the amount of fibres and distribution across the block. The formation and progression of cracks can be seen during the T series and P series tests, while for the C series, the crack exhibits sudden formation and evolution (Fig. 5), as confirmed by the values of E_1, E_2 and E_3. All failures paths are located in the middle section for all samples; no exceptions are observed, probably due to the stress concentration introduced by the steel cylinder in the middle of the earth block.

3.2. Elaboration of the bending tests data

To calculate the maximum tensile stress of the earth blocks, two models were considered: (i) the elastic De Saint Venant model and (ii) the Strut and Tie model. Based on the first one, which consists of an elastic beam of length d=240 mm, thickness b=140 mm and height h=95 mm, the classic strength modulus W_{el} and the maximum tensile stress σ_1 are:

$$W_{el} = \frac{bh^2}{6}; \qquad \sigma_1 = \frac{P\,d}{4W_{el}} \tag{1}$$

where P is the applied load. This formulation is derived from UNI 1051-11: 2007, in which the tensile stress is expressed by:

$$\sigma_1 = 1.5\frac{Pd}{bh^2}. \tag{2}$$

Considering the ISCEB as a Strut and Tie scheme, with an equivalent symmetric truss with two compressed rods inclined such that tgθ=2h/d with respect to the horizontal, the horizontal tensile force H on the trussed element is:

$$H = \frac{Pd}{4h}. \tag{3}$$

Supposing a uniform stress distribution, the resultant force operates at $h' = \frac{h}{5}$ from the lower face of the unit; thus, the thickness of the tensile fibre is $t = h'$. The tensile stress conventionally furnished by this model is:

$$\sigma_2 = \frac{H}{tb}. \tag{4}$$

The numerical results of both models are listed in Table 5.

3.3. Discussion of bending test results

Table 5 and Table 6 summarize the average and standard deviations of all data obtained from the bending tests. Despite the simplicity of the adopted approaches, the results in terms of bending tensile strength are in mutual agreement. Indeed, for each series of blocks, the average and standard deviation values calculated using the two methods are similar, with a maximum difference of approximately 19% for the PSNF type and a minimum difference of 15% for the TXF type. The Strut and Tie method overestimates the values of the flexural tensile stresses compared to the De Saint Venant method, as expected. Indeed, the latter involves a flexural mechanism, in which the internal lever arm is lower than that of the Strut and Tie method. Specifically, a rectangular cross-section has an internal lever arm equal to 2/3 of the depth h, whereas in the Strut and Tie method, it is approximately 80% of the depth. Consequently, the results of the Strut and Tie method can be considered as upper bounds of the real stresses, whereas those of the De Saint Venant method can be regarded as lower bounds.

Both methods provide a quick comparison of results, offering a simple and repeatable method for calculation, which is useful for producers of ISCEBs, when similar experimental results are available.

It should also be noted that the geometry of the sample (i.e., the presence of holes) did not influence the crack surfaces during the three-point bending test, as shown in Fig. 5.

Table 5. Strength data from three-point bending tests

	Mean	Standard Deviation		Mean	Standard Deviation		Mean
	$x(F_{max})$ (mm)	F_{max} (kN)		$x(F_{max})$ (mm)	F_{max} (kN)		$x(F_{max})$ (mm)
TWF	0.51	0.73	0.21	0.25	0.06	0.02	0.02
TXF	0.86	0.97	0.28	0.33	0.1	0.03	0.04
TWNF	0.74	0.85	0.24	0.29	0.04	0.01	0.02
TXNF	0.81	0.92	0.26	0.31	0.08	0.03	0.02
CWF	1.12	1.66	0.47	0.57	0.14	0.04	0.04
CXF	1.24	2.75	0.78	0.94	0.38	0.12	0.13
CWNF	0.98	2.18	0.62	0.75	0.31	0.1	0.11
CXNF	1.01	2.6	0.74	0.89	0.23	0.07	0.08
PSF	0.75	0.73	0.21	0.25	0.06	0.02	0.02
PWF	1.2	0.89	0.25	0.3	0.07	0.02	0.02
PSNF	0.75	0.78	0.22	0.27	0.07	0.02	0.02
PWNF	0.95	0.96	0.27	0.33	0.12	0.04	0.04

x = displacement; Fmax = load; σ^1_{max}= De Saint Venant stress; σ^2_{max} = Strut and Tie stress
T= only soil; P = with straw fibers; C = with lime
S = reduced mass (6.4 kg); W = normal mass (6.6 kg); X = superior mass (6.8 kg)
F = bi-direct. compaction; NF = mono-direct. Compaction.

Table 6. Energy density parameters from three points bending tests

	E_1 (MPa)	E_2 (MPa)	E_3 (MPa)	p_1	p_2	λ
TWF	0.19	0.06	0.18	0.41	0.30	1.61
TXF	0.50	0.03	0.03	0.05	0.47	0.11
TWNF	0.41	0.01	0.01	0.02	0.49	0.04
TXNF	0.46	0.02	0.03	0.04	0.43	0.12
CWF	0.78	0.01	0.01	0.01	0.28	0.03
CXF	1.08	0.01	0.01	0.01	0.12	0.02
CWNF	0.82	0.01	0.02	0.02	0.15	0.05
CXNF	0.88	0.00	0.00	0.00	0.00	0.00
PSF	0.28	1.25	4.33	4.80	0.22	21.39
PWF	0.66	1.44	4.65	2.31	0.24	9.71
PSNF	0.35	0.85	2.74	2.50	0.24	10.75
PWNF	0.50	0.67	2.64	1.54	0.20	7.57

T= only soil; P = with straw fibers; C = with lime
S = reduced mass (6.4 kg); W = normal mass (6.6 kg); X = superior mass (6.8 kg)
F = bi-direct. compaction; NF = mono-direct. Compaction

The following considerations can be finally made:

1) The C series exhibited the highest values of strength and ultimate displacement (Table 5), though this does not imply relevant ductility, as shown by the E_1 and E_2 parameters (Table 6). Indeed, the accumulated elastic energy was dissipated via an instantaneous crack with substantial brittle behaviour. In contrast, the P series exhibited lower strength (Table 5) but considerable ductility and dissipated energy due to the reinforcement role of the fibres (Table 6). Fig. 5 shows how the straw fibres introduced a mechanical component able to provide flexural strength to the unit.
2) Considering the same type of compaction and mixture, i.e., F-NF and T-C-P, respectively, the increase in mass of the units (S-W-X) enhanced both strength and stiffness together with the elastic energy but implied a ductility reduction.
3) For the same mixture (T-C-P series) and mass (W-X-S series), the compaction modality (mono- or bi-directional) did not produce an increase in tensile strength but generally enhanced the maximum displacements.
4) The increase in tensile strength and its displacement associated with the P or C series compared to the T series (only soil) caused a different mechanical response: the addition of straw fibres did not cause a remarkable increase in strength (approximately 17%), while the addition of lime (C series) significantly strengthened the blocks (approximately 150%). In contrast, the fibres

induced a relevant increase in displacements (125%) when accompanied by bi-directional floating compaction. Also, with the addition of lime, bi-directional floating compaction produced a larger increase in displacements.

4. Compression tests

4.1. Setup of the compression tests

The resulting pairs of half specimens obtained from the bending tests were subjected to compression tests. Displacement-controlled compression tests were carried out using the same Instron model 1186 machine with a displacement rate of 0.5 mm/min and a full-scale force of 5000 daN. The displacement of the middle section of the blocks was recorded using two potentiometers (tolerance: 1 □m) on the far end of the crossbeam, and the data were elaborated using the Scilab-5.5.2 software. Because the maximum difference between the values of the two potentiometers was less than 0.1 mm, the average displacements were calculated in this case as well. An analogous calibration ensured negligible displacements of the faces of the specimen with respect to the extremities of the strain gages, using the same measuring device shown in Fig. 3.

The tests showed an adjustment between the machine and the block for loads up to 100 daN; thus, the initial part of the diagram was not plotted. Fig. 4b presents a typical diagram of specimen CEB71 of the PSNF series. The compression force-displacement diagram of each block was evaluated as the average values of both parts of the block given by its flexural collapse. The maximum strength C_{max} and the relative displacement $x(C_{max})$ of each specimen are highlighted. Since the blocks revealed a negligible residual strength for high displacement values after the peak, the ultimate strength was conventionally assumed to be $0.3C_{max}$ with the corresponding displacement $x_{c,u}$. The same energy terms ($E_{c,1}$, $E_{c,2}$, $E_{c,3}$) and parameters ($p_{c,1}$, $p_{c,2}$, λ_c) defined for the bending tests were also used for the compression tests.

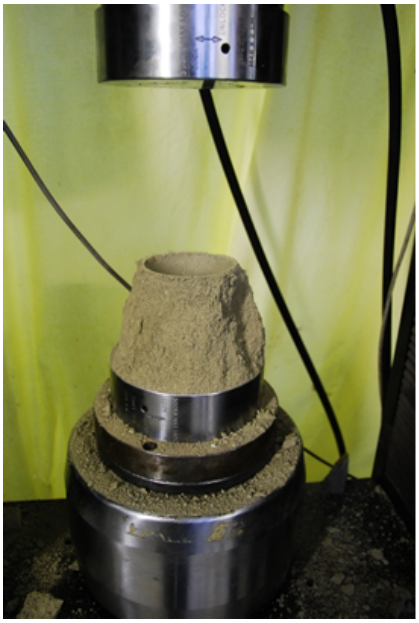

Fig. 6. Compression failure of C series with detail of cone shaped crack surface

For all the tests, the data dispersion was limited, and the crack surface created a conical section affecting the portion around the hole, in agreement with the Coulomb failure theory (Fig. 6). With respect to the other samples, only in the P series did the slivers exhibit tensile resistance, reconfirming the reinforcing role of the fibres regarding the tensile strength value.

4.2. Results of the compression test

The compression strength due to the compression force C was calculated by considering both the area without holes A and the area with holes A_h, which are given, respectively, by:

$$\sigma_A = \frac{C}{A} \tag{5}$$

$$\sigma_{A_h} = \frac{C}{A_h} \tag{6}$$

Table 7 and Table 8 contain the average and standard deviations of all the results. One can observe that the presence of straw fibres (P series) ensures a containment effect due to the tensile strength of the fibres, which increase the unit bearing capacity. This observation confirms, in regards to the bearing capacity, the evidence supporting the traditional empirical practice of adding straw fibres to earth blocks.

4.3. Discussion of the compression test results

It should be noted that, similar to the bending tests, the sample geometry did not influence the crack surfaces, as shown in Fig. 6. The following considerations can be made.

1) The C series exhibits the highest compression strength, while the failure displacement values of the T and C series are comparable.
2) Higher collapse displacement values are obtained for the P series, which also exhibits the highest elastic and plastic energies.
3) For the same compaction modality and mixture (N-NF and T-C-P series, respectively), an increase in mass caused an expected increase in maximum strength but an unexpected increase in relative displacement and elastic energy.
4) For the same mixture (T-C-P series) and mass (W-X-S series), the compaction modality does not imply a significant improvement in tensile strength. With a few exceptions, there is a relationship of direct proportionality between compaction force and compression strength.
5) The increases in compression strength and its associated displacement compared to the T series (only soil) are higher when lime is used in place of the fibres. In contrast, relevant increases in displacement, with respect to lime, occur due to the addition of fibres. This allows detection of the role of additives in the mechanical performances of the blocks.

No relevant differences between floating and non-floating compaction, in terms of strength or displacements with the same mass, were obtained, although the compression strength appeared to be directly proportional to the compacting force during the production of ISCEBs. In other words, the compaction modality influences the strength of the units via their increases in mass.

5. Final discussion and conclusions

This paper presented results from experiments on earth blocks with three distinct mixtures (earth, earth and lime, earth and straw) obtained using a human-powered machine named Float RAM 1.0 Press. This manufacturing procedure was used to produce handcrafted interlocking stabilized compressed earth blocks (ISCEBs). Three-point bending tests and uniaxial compression tests were carried out to investigate the mechanical behaviour of ISCEBs. The improvements obtained by incorporating additives were illustrated and discussed. Based on the obtained data, the proposed manual procedure for producing earth blocks is very reproducible with significant reliability. An interesting production parameter was achieved using the proposed manual press: a daily production of approximately 240 units, i.e., a single leaf wall of approximately 6 to 7 m^2, can be achieved via a process requiring low levels of embodied construction energy. The uniform quality of production, in terms of the mechanical parameters, was shown to be high. Only the addition of natural fibres yielded some unpredictability in

quality control. This is caused by the difficulty in controlling the distribution of fibres in a mixture during manual production. The compaction modality influenced the mechanical properties of the ISCEBs in terms of increasing the bearing capacity as the mass of the units was increased. The best results for bi-directional floating compaction were obtained with mixtures containing straw fibres. Although, the compaction force on the upper plate during production was higher in the case of a floating mould, the maximum compaction force increased with the mass introduced in the mould, particularly when straw fibres were added. In that case, the addition of fibres decreases the density; thus, the volume to be compacted is increased, assuming a constant block mass.

The addition of lime increased the flexural tensile strength of the block and the corresponding collapse deformation. Nevertheless, a brittle collapse occurred, as indicated by the values of dissipated energy reported in Table 5. The addition of fibres ensured a higher ultimate displacement, conferring a significant ductility to the ISCEBs. In all specimens, the increase in flexural capacity corresponded to an increase in mass. Moreover, the ductility decreased, highlighting the relationship between brittle behaviour and the density of ISCEBs.

Table 7. Strength data from compression tests

	Mean	Standard Deviation		Mean	Standard Deviation		Mean
	$x(C_{max})$ (mm)	C_{max} (kN)		$x(C_{max})$ (mm)	C_{max} (kN)		$x(C_{max})$ (mm)
TWF	1.17	16.35	0.83	1.10	2.91	0.15	0.20
TXF	1.24	21.19	1.08	1.43	1.18	0.06	0.08
TWNF	1.06	17.15	0.88	1.16	0.63	0.03	0.04
TXNF	1.16	19.51	1.00	1.32	0.92	0.05	0.06
CWF	1.14	27.71	1.41	1.87	1.75	0.09	0.12
CXF	1.32	34.74	1.77	2.34	3.05	0.16	0.21
CWNF	1.24	28.89	1.47	1.95	1.42	0.07	0.10
CXNF	1.26	36.64	1.87	2.47	2.04	0.10	0.14
PSF	1.78	14.34	0.73	0.97	2.65	0.14	0.18
PWF	2.37	18.20	0.93	1.23	0.84	0.04	0.06
PSNF	1.85	15.06	0.77	1.02	1.20	0.06	0.08
PWNF	1.97	17.60	0.90	1.19	0.67	0.03	0.05

x = displacement; C_{max} = load; $\sigma_A = C_{max}/A$; $\sigma_{Ah} = C_{max}/A_h$
T= only soil; P = with straw fibers; C = with lime
S = reduced mass (6.4 kg); W = normal mass (6.6 kg); X = superior mass (6.8 kg)
F = bi-direct. compaction; NF = mono-direct. Compaction.

The compression tests revealed a cone-shaped crack surface corresponding to the classic Coulomb theory. The addition of lime considerably improved the compression strength, as shown in Table 7. The addition of natural fibres caused interesting values of the ductility factor in terms of energy, confirming their reinforcement role. The entire set of experimental data is presented in (Romanazzi, 2016). However, the real geometry of ISCEBs was not considered in the mechanical analysis, which focused on the overall strength and displacements. For this reason, further assessment via the FEM can better reveal the stress distribution in a block. Additional investigations related to the study of straw fibres with a procedure to ensure uniform distribution of the stresses in manual production can be carried out.

Table 8. Energy density parameters from compression tests

	E_1 (MPa)	E_2 (MPa)	E_3 (MPa)	p_1	p_2	λ
TWF	10.79	8.63	12.81	0.81	0.40	2.01
TXF	14.95	11.85	17.68	0.80	0.40	1.99
TWNF	10.44	8.03	12.50	0.77	0.39	1.96
TXNF	12.49	10.58	15.59	0.85	0.40	2.11
CWF	17.74	14.23	21.63	0.81	0.40	2.04
CXF	23.91	21.63	32.98	0.92	0.39	2.34
CWNF	19.66	15.14	23.81	0.77	0.39	1.99
CXNF	25.73	21.05	32.46	0.82	0.40	2.08
PSF	15.03	18.05	27.60	1.33	0.40	3.34
PWF	22.35	23.36	35.58	1.04	0.40	2.64
PSNF	15.96	23.63	36.87	1.49	0.39	3.80
PWNF	18.96	20.70	32.62	1.09	0.39	2.81

T= only soil; P = with straw fibers; C = with lime
S = reduced mass (6.4 kg); W = normal mass (6.6 kg); X = superior mass (6.8 kg)
F = bi-direct. compaction; NF = mono-direct. compaction

Finally, regarding seismic risk, the aspect of out-of-plane stability should be evaluated, taking into account the geometrical ratios (Laursen et al., 2015) and rocking behaviour (Giresini et al., 2017), with the aim to evaluate the ability to dissipate energy during rocking motion, which is a crucial aspect of seismic analysis.

Acknowledgements

This research was supported by the RELUIS Consortium (Masonry division), sponsored by the Italian DPC government agency.

References

Andreini, M., De Falco, A., Giresini, L., & Sassu, M. (2013). Structural analysis and consolidation strategy of the historic Mediceo Aqueduct in Pisa (Italy). *In Applied Mechanics and Materials (Vol. 351, pp. 1354-1357). Trans Tech Publications*.

Anifowose, A. Y. B. (2000). Stabilisation of lateritic soils as a raw material for building blocks. *Bulletin of Engineering Geology and the Environment, 58*(2), 151-157.

Arumala, J. O., & Gondal, T. (2007). Compressed earth building blocks for affordable housing. *In The construction and building research conference of the Royal Institution of Chartered Surveyors*.

Bati, B. (2001). Natural additives for improving the mechanical properties and durability of adobe building material. *Materials Engineering, 12*(3), 413-425.

Billong, N., Melo, U. C., Louvet, F., & Njopwouo, D. (2009). Properties of compressed lateritic soil stabilized with a burnt clay–lime binder: effect of mixture components. *Construction and Building Materials, 23*(6), 2457-2460.

Binici, H., Aksogan, O., & Shah, T. (2005). Investigation of fibre reinforced mud brick as a building material. *Construction and Building Materials, 19*(4), 313-318.

Binici, H., Aksogan, O., Bodur, M. N., Akca, E., & Kapur, S. (2007). Thermal isolation and mechanical properties of fibre reinforced mud bricks as wall materials. *Construction and Building Materials, 21*(4), 901-906.

Bouhicha, M., Aouissi, F., & Kenai, S. (2005). Performance of composite soil reinforced with barley straw. *Cement and Concrete Composites, 27*(5), 617-621.

Bruno, A. W., Gallipoli, D., Perlot, C., & Mendes, J. (2017). Mechanical behaviour of hypercompacted earth for building construction. *Materials and Structures, 50*(2), 160.

Bui, Q. B., Morel, J. C., Hans, S., & Meunier, N. (2009). Compression behaviour of non-industrial materials in civil engineering by three scale experiments: the case of rammed earth. *Materials and Structures, 42*(8), 1101-1116.

Delgado, M. C. J., & Guerrero, I. C. (2006). Earth building in Spain. *Construction and building materials, 20*(9), 679-690.

Ferraresi, C., Franco, W., & Quaglia, G. (2011, January). Human powered press for raw earth blocks. *In ASME 2011 International Mechanical Engineering Congress and Exposition (pp. 579-588). American Society of Mechanical Engineers*.

Ferraresi, C., Franco, W., & Quaglia, G. (2014). Float-ram: a new human powered press for earth blocks.

Franco, W., Iarussi, F., & Quaglia, G. (2016). Human powered press for producing straw bales for use in construction during post-emergency conditions. *Biosystems Engineering, 150*, 170-181.

Franco, W., Quaglia, G., & Ferraresi, C. (2017). Experimentally based design of a manually operated baler for straw bale construction. *In Advances in Italian Mechanism Science (pp. 307-314). Springer, Cham*.

Giresini, L. (2016). Energy-based method for identifying vulnerable macro-elements in historic masonry churches. *Bulletin of Earthquake Engineering, 14*(3), 919-942.

Giresini, L., & Sassu, M. (2017). Horizontally restrained rocking blocks: evaluation of the role of boundary conditions with static and dynamic approaches. *Bulletin of Earthquake Engineering, 15*(1), 385-410.

Giresini, L., Fragiacomo, M., & Sassu, M. (2016). Rocking analysis of masonry walls interacting with roofs. *Engineering Structures, 116*, 107-120.

Gomes Battistelle, R. A., & Borges Faria, O. (2005). Aproveitamento do lodo residual do proceso de fabricação de celulose e papel em tijolos de terra-crua. In Terra em Seminário (pp. p-237). Argumentum.

Guettala, A., Houari, H., Mezghiche, B., & Chebili, R. (2002). Durability of lime stabilized earth blocks. *Courrier du Savoir, 2*(1), 61-66.

Houben, H., & Guillaud, H. (1989). Traité de construction en terre. Editions Parenthèses.

Houben, H., & Guillaud, H. (1994). *Earth Construction: A Comprehensive Guide*. Intermediate Technology Publications.

Kouakou, C. H., & Morel, J. C. (2009). Strength and elasto-plastic properties of non-industrial building materials manufactured with clay as a natural binder. *Applied Clay Science, 44*(1-2), 27-34.

Laursen, P. T., Herskedal, N. A., Jansen, D. C., & Qu, B. (2015). Out-of-plane structural response of interlocking compressed earth block walls. *Materials and Structures, 48*(1-2), 321-336.

Lenci, S., Piattoni, Q., Clementi, F., & Sadowski, T. (2011). An experimental study on damage evolution of unfired dry earth under compression. *International journal of fracture, 172*(2), 193-200.

Maskell, D., Reddy, V., Heath, A., & Walker, P. (2016). Modern earth construction techniques–an overview. *In 16th International Brick and Block Masonry Conference, 2016. University of Bath*.
Matta, F., Cuéllar-Azcárate, M. C., & Garbin, E. (2015). Earthen masonry dwelling structures for extreme wind loads. *Engineering Structures, 83*, 163-175.
Mattone, R. (2001). Unfired earth, traditions and innovations. *Ind. Laterizi, 12*(71), 313-320.
Melo, A. B., Barbosa, N. P., Lima, M. R. F., & Silva, E. P. (2011). Structural performance for a masonry prototype built with blocks of stabilized raw earth. *Ambiente Construído, 11*(2), 111-124.
Millogo, Y., Aubert, J. E., Hamard, E., & Morel, J. C. (2015). How properties of kenaf fibers from Burkina Faso contribute to the reinforcement of earth blocks. *Materials, 8*(5), 2332-2345.
Morel, J. C., & Pkla, A. (2002). A model to measure compressive strength of compressed earth blocks with the '3 points bending test'. *Construction and Building Materials, 16*(5), 303-310.
Morel, J. C., Pkla, A., & Walker, P. (2007). Compressive strength testing of compressed earth blocks. *Construction and Building Materials, 21*(2), 303-309.
Mukerji, K. (1988). Soil block presses. *Eschborn, Federal Republic of Germany, German Appropriate Technology Exchange*.
Niroumand, H., Zain, M. F. M., & Jamil, M. (2013). Various types of earth buildings. *Procedia-Social and Behavioral Sciences, 89*, 226-230.
Oliveira, D. V., Miranda, T. F., Ramos, L. F., Silva, R. A., Soares, E., & Leitão, D. (2016). Mechanical performance of compressed earth block masonry using granitic residual soils. *In IB2MAC, 16th International Brick and Block Masonry Conference. Taylor & Francis*.
Oppong, R. A., & Badu, E. (2012). Evaluation of Stabilised-Earth (Tek) Block for Housing Provision and Construction in Ghana. *Journal of Science and Technology (Ghana), 32*(2), 104-118.
Osula, D. O. A. (1996). A comparative evaluation of cement and lime modification of laterite. *Engineering geology, 42*(1), 71-81.
Pacheco-Torgal, F., & Jalali, S. (2012). Earth construction: Lessons from the past for future eco-efficient construction. *Construction and Building Materials, 29*, 512-519.
Parisi, F., Asprone, D., Fenu, L., & Prota, A. (2015). Experimental characterization of Italian composite adobe bricks reinforced with straw fibers. *Composite Structures, 122*, 300-307.
Pekmezci, B. Y., KAFESÇİOĞLU, R., & Agahzadeh, E. (2012). Improved performance of earth structures by lime and gypsum addition. *METU JFA, 2*, 205.
Qu, B., Stirling, B. J., Jansen, D. C., Bland, D. W., & Laursen, P. T. (2015a). Testing of flexure-dominated interlocking compressed earth block walls. *Construction and Building Materials, 83*, 34-43.
Qu, B., Stirling, B. J., Laursen, P. T., & Jansen, D. C. (2015b). Analysis and seismic performance evaluation of flexure-dominated interlocking compressed earth block walls. *Advances in Structural Engineering, 18*(12), 2167-2179.
Reddy, B. V. (2015). Design of a manual press for the production of compacted stabilized soil blocks. *Current Science (00113891), 109*(9), 1651-1659.
Romanazzi, A. (2016). Interlocking stabilized compressed earth blocks: production, mechanical behavior and design of school in Burkina Faso. (Italian) MSc Thesis, School of Engineering, tutors M. Sassu, L. Lanini, E. Orefice, University of Pisa.
Sassu, M., De Falco, A., Giresini, L., & Puppio, M. L. (2016a). Structural solutions for low-cost bamboo frames: Experimental tests and constructive assessments. *Materials, 9*(5), 346.
Sassu, M., Giresini, L., Bonannini, E., & Puppio, M. L. (2016b). On the use of vibro-compressed units with bio-natural aggregate. *Buildings, 6*(3), 40.
Silva, R. A. M., Soares, E., Oliveira, D. V., Miranda, T. F., Cristelo, N., & Oliveira, J. V. (2015, June). CEBs stabilised with geopolymeric binders: mechanical performance of dry-stack masonry. *In WASCON 2015-9th International Conference on the Environmental and Technical Implications of Construction with Alternative Materials* (pp. 1-6).
Sturm, T., Ramos, L. F., & Lourenço, P. B. (2015). Characterization of dry-stack interlocking compressed earth blocks. *Materials and Structures, 48*(9), 3059-3074.
Varadarajan, R., & Govindan, V. (2013). Experimental analysis to utilize the solid wastes in brick production. *Journal of Environmental Science & Engineering, 55*(3), 343-350.
Venkatarama Reddy, B. V., Suresh, V., & Nanjunda Rao, K. S. (2016). Characteristic compressive strength of cement-stabilized rammed earth. *Journal of Materials in Civil Engineering, 29*(2), 04016203.
Walker, P. J. (1995). Strength, durability and shrinkage characteristics of cement stabilised soil blocks. *Cement and Concrete Composites, 17*(4), 301-310.